UNIVERSITY OF SPLIT
FACULTY OF ELECTRICAL ENGINEERING, MECHANICAL ENGINEERING AND NAVAL ARCHITECTURE

POSTGRADUATE DOCTORAL STUDIES MECHANICAL ENGINEERING

QUALIFYING EXAM

Propellant Sloshing Control in Microgravity

Ines Bezić

Split, September 2026.

Contents

1. Introduction

Liquid motion in moving containers is important for designing safer vehicles, ships and structures. When liquids slosh inside partially filled tanks, the resulting motion directly disturbs vehicle dynamics. This issue is well known in many engineering areas, including aircraft and rocket fuel tanks design, construction of ships, and other vehicles. [1–3] Sloshing can produce unsteady forces and overturning moments on the tank structure, directly impacting vehicle center of mass and movement. [4] On Earth, gravity regulates sloshing, the hydrostatic pressure gradient pulls displaced liquid back toward a flat equilibrium, while surface tension acts only as a local correction near the tank walls [1, 2]. In orbit, effective acceleration drops to microgravity levels (10^{-6} to $10^{-3}g$), causing gravitational body forces weaken while surface tension takes over [5–8]. In the regime where Bond number is low ($Bo \leq 1$), capillary forces may become greater than gravitational forces [9–11]. Therefore, inertia remains important to the liquid's dynamic response, while viscous effects contribute to energy dissipation and damping. Instead of a flat interface form, liquids climb along tank walls, entrap gas bubbles, and reorient under spacecraft maneuvers [12, 13], which can cause pressure drops in cryogenic tanks [14]. Since flat-interface models assume Earth gravity condition, their assumptions to predict fluid motion under microgravity may become inadequate [15, 16]. Managing low-gravity slosh has therefore grown into a multidisciplinary field that connects capillary hydrodynamics, structural dynamics, precision control theory, and active actuation [17–19].

Flight records document several critical instances of sloshing behaviour. During the Apollo 11 lunar module descent, slosh-induced orientation drift has repeatedly complicated engine restarts and increased propellant consumption [5, 20–22]. This issue has motivated the characterization of slosh dynamics behaviour across flight regimes, using both experimental tests and numerical simulations [23, 24]. Studies analyse sloshing behaviour in spherical tanks test with water and liquid nitrogen [25], cryogenic propellant sloshing in pressurized cylindrical tanks [26], analytical analysis of in-space propellant storage [27], and large scale hydrogen slosh testing [28]. In parallel, Eulerian VOF-based approaches and Lagrangian SPH methods have been used as reliable tool for sloshing behaviour studies [29–36]. Lagrangian differencing dynamics method is implemented with Rhoxyz solver developed by Bašić et al. [37]. The computational domain is represented with moving points cloud. The solver is GPU-accelerated, which makes it efficient for free surface sloshing problems. LDD setup is based on 2nd order gradient and Laplacian approximations derived from Taylor expansion with Lanson and Vila scheme [38]. Together, these experimental and numerical studies have improved predictions of the sloshing disturbance and damping behaviour in tanks.

This review examines the physical mechanisms, passive devices, and active control methods developed for microgravity sloshing. The methodology follows fundamentals analysis of the main microgravity dimensionless parameters and the equivalent mechanical models. Passive and active sloshing control technologies were reviewed, along with the vibro-acoustics phenomena.

Section 2 examines capillary hydrodynamics, contact-line mechanics, and equivalent mechanical models used in flight control. Section 3 reviews passive technologies, including ring baffles, damping equations, surface-tension propellant management devices (PMDs), and tuned liquid dampers. Section 4 explores active control strategies, covering force-feedback platforms, mobile baffles, magnetic ferrofluid positioning, piezoelectric transducers, and coupled spacecraft attitude control laws. Section 5 discusses acoustic radiation pressure, ultrasonic manipulation, Faraday waves, and the distinction between structural acoustics and fluid interface actuation. Final section brings conclusion, key research gaps and presents a research proposal for acoustic slosh control. Figure 1.1 shows flow chart of the report structure.

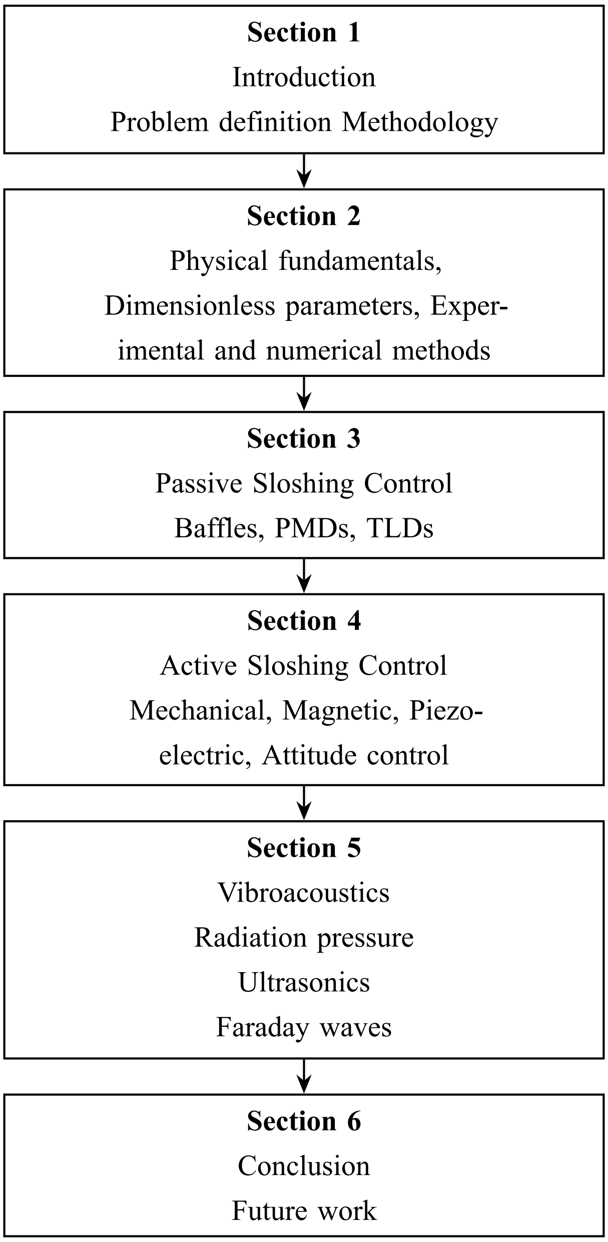

Figure 1.1. Flow Diagram of the Report Structure.

2. Physical Fundamentals

2.1. Microgravity Hydrodynamics

Liquid sloshing dynamics has been the major aerospace engineering concern starting in the early 1960s. Since then, numerous experimental and theoretical studies of liquid sloshing have been published. Dodge et al. [6] analyses and compares experiments with liquid sloshing in a rigid cylindrical tank under small axial accelerations conditions. Their theory is valid for Bond numbers larger than 10, finding good correlation for the sloshing forces and natural frequency as a Bond number function. The Bond number (Bo) is a dimensionless number that gives correlation between gravitational and surface tension forces:

$$\mathrm{Bo} = \frac{\Delta\rho\, g\, L^2}{\gamma}. \tag{2.1}$$

where $\Delta\rho$ is difference in density of two phases, g is gravitational acceleration, L is characteristic length, and γ is the surface tension [6, 9]. Cassoni [9] analysed curvature-corrected sloshing spectra for cylindrical tanks in microgravity conditions showing that equilibrium curvature couples radial modes and alters the low order spectrum once $Bo \lesssim 1$. The Concus-Finn condition [11] explains spontaneous liquid rise and wetting in sharp corners or capillary channels (see Fig. 2.1). They characterized the surface with the mean curvature proportional to its height above a reference plane. Concluding that the qualitative behaviour of such a surface near the vertex changes markedly. Other significant dimensionless parameters are given in Table 2.1.

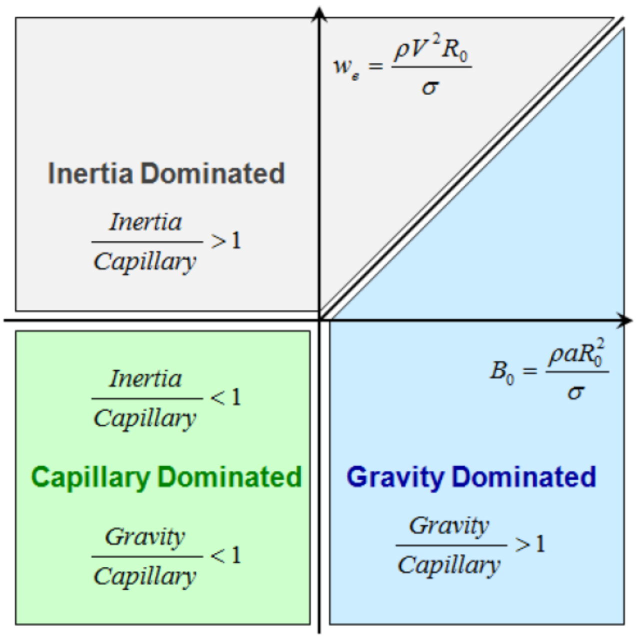

Figure 2.1. Hydrodynamic Regimes [39]

Dodge and Garza [6–8] studied low gravity sloshing in spherical and cylindrical tanks with inverted bottoms, emphasizing the liquid depth variation effect and smooth wall damping determination. Results showed that the variation in free surface curvature with liquid depth strongly effects the natural frequency. Also, the damping is shown to be minimal when the tank is half full. Figure 2.2 [8] shows that the same Bond number might have different effects for different liquid levels.

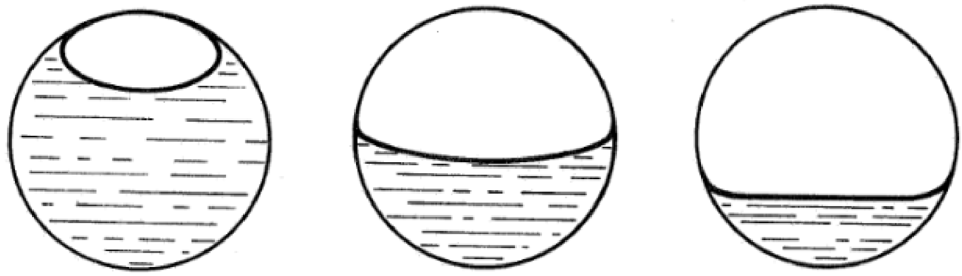

Figure 2.2. Different Surface Curvature for the Different Fill Levels [8]

Utsumi [10] introduced a partial spherical coordinate system (see Fig. 2.3) and evaluated the meniscus and liquid sloshing in an axisymmetric container. The axisymmetric meniscus M and the liquid surface F are expressed by:

$$M : z = z_M(r) \tag{2.2}$$

$$F : \quad z = z_F(r, \varphi, t) = z_M(r) + \eta(r, \varphi, t), \tag{2.3}$$

where η is the liquid surface elevation.

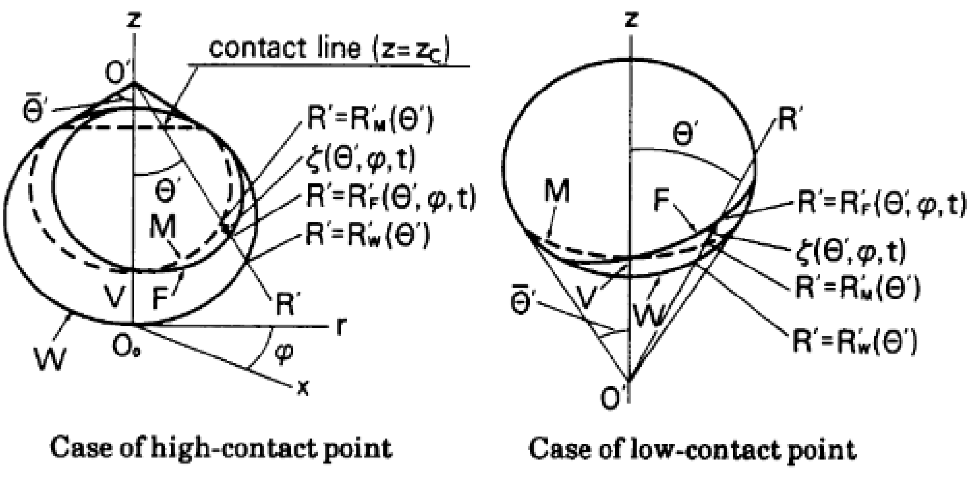

Figure 2.3. Spherical Coordinate Systems $O' - R'\theta'\varphi$ [10]

Utsumi [10] also shows the connection between Bond number and natural frequencies increase with the increase of the liquid filling level, when the Bond number is small, the surface tension is dominant comparing to the gravity. Figure 2.4 shows slosh frequencies ω_m, where m is circumferential wave number, and curves numerals indicate $\log_{10} B_O$.

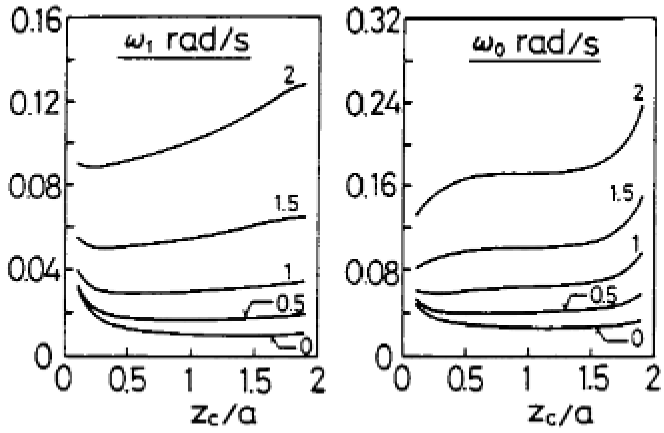

Figure 2.4. Slosh Frequencies [10]

Dalmon et al. [12] compared direct numerical simulations with the FLUIDICS experiment on the International Space Station, verifying that capillary oscillations in spherical tanks produce distinct force and moment signatures tied directly to the 3D meniscus shape. Li et al. [13] investigated the dynamic behaviour of free surface using volume of fluid (VOF) method in a context of dynamic contact angle (DCA) model. It shows that dynamic deflections of meniscus reveal dependency between oscillation frequency of free surface and the contact line boundary condition. The damping ratio of microgravity sloshing is larger than the normal-gravity sloshing. For the space vehicle dynamics analysis, a correction for the phase lag is required [40, 41].

Table 2.1. Dimensionless Parameters and their Physical Significance

Parameter	**Mathematical Expression**	**Physical Significance**
Bond Number (Bo)	$\text{Bo} = \frac{\Delta\rho\, g\, L^2}{\gamma}$	$\frac{\text{Gravitational Body Forces}}{\text{Surface Tension (Capillary) Forces}}$
Reynolds Number (Re)	$\text{Re} = \frac{\rho\, U\, L}{\mu}$	$\frac{\text{Inertial Forces}}{\text{Viscous Forces}}$
Weber Number (We)	$\text{We} = \frac{\rho\, U^2\, L}{\gamma}$	$\frac{\text{Inertial Forces}}{\text{Surface Tension Forces}}$
Ohnesorge Number (Oh)	$\text{Oh} = \frac{\mu}{\sqrt{\rho\, \gamma\, L}} = \frac{\sqrt{\text{We}}}{\text{Re}}$	$\frac{\text{Viscous Forces}}{\sqrt{\text{Inertial} \times \text{Surface Tension Forces}}}$
Froude Number (Fr)	$\text{Fr} = \frac{U}{\sqrt{g\, L}}$	$\frac{\text{Inertial Forces}}{\text{Gravitational Forces}}$
Capillary Number (Ca)	$\text{Ca} = \frac{\mu\, U}{\gamma} = \frac{\text{We}}{\text{Re}}$	$\frac{\text{Viscous Forces}}{\text{Surface Tension Forces}}$
Damping Parameter (δ)	$\delta = \frac{2\nu}{\omega}$	$\frac{\text{Acoustic / Viscous Boundary Layer Thickness}}{\text{Tank Characteristic Radius}}$

2.2. Equivalent Mechanical Models

Jang et al. [39] and Capolupo [42] presented the mechanical slosh model which contains of a rigid mass and a mass-spring-damper model (see Figs. 2.5 and 2.6). Abramson et al. [1, 2, 15] established the standard analytical framework for these models by solving the linear potential flow problem for moving containers. Slosh forces and moments can be modelled as a fixed mass m_0 combined with a set of modal pendulums or mass-spring-damper oscillators. The Laplace transformed mechanical slosh model can be mathematically formulated as:

$$m_n(s^2 + 2\zeta_n\omega_n s + \omega_n^2)Z_n = f_{rs} + f_{fs} \tag{2.4}$$

where m_n (mass), ω_n (frequency), ζ_n (damping), and Z_n (location) are functions of the physical properties of the space tank liquid, the liquid level, the tank radius, and the axial body force.

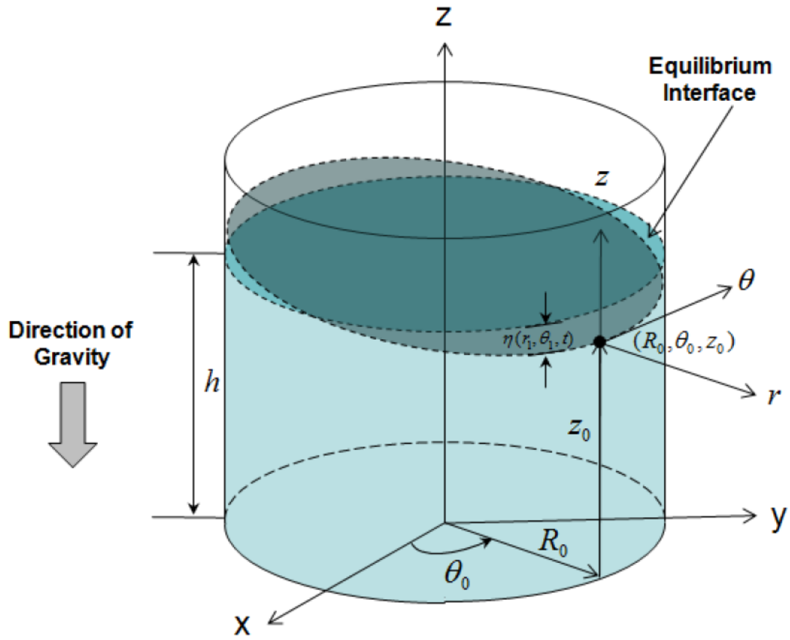

Figure 2.5. Equilibrium of Liquid Surface [39]

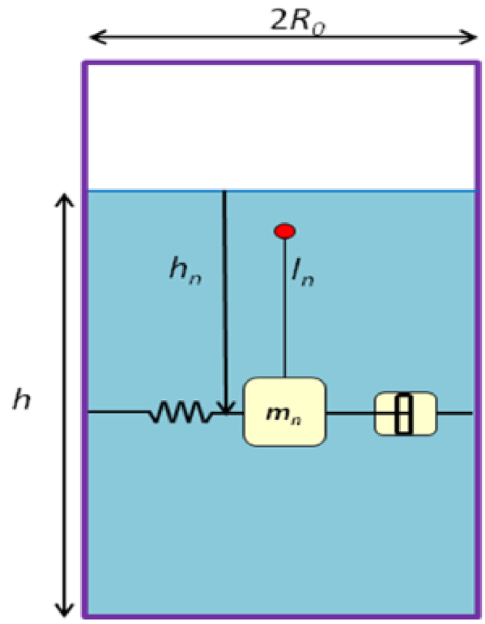

Figure 2.6. Mechanical Models of Sloshing for a Cylindrical Tank [39]

Graham [43] and Graham and Rodriquez [44] derived equivalent spring–mass formulations for rectangular tanks, providing the analytical basis for early flight control analysis. Utsumi [10, 45, 46] developed equivalent mechanical models for low-gravity containers under lateral and axial excitation by incorporating capillary potential energy directly into the pendulum equations. Utsumi [47], Abramson et al. [15], and Gao et al. [48] captured torsional stiffness and membrane constraints for specific tank designs. Kana [49] developed a compound pendulum model to predict rotary liquid slosh in a scale model, predicting a significant magnitude cross-axis force which was not predicted by the usual linear theory models. Farid and Gendelman [50] identified internal resonances between fundamental and higher-order antisymmetric modes. Miao et al. [51, 52] formulated nonlinear mechanical models for spherical tanks to capture severe interface reorientation. To calibrate these reduced-order models for complex tank geometries, Yang and Peugeot [53] introduced CFD-based parameter extraction workflows. By applying known kinematic pulses to a CFD tank simulation, engineers extract pendulum mass, hinge height, and damping coefficients directly from force histories, supplying GNC systems with verified plant models.

2.3. Experimental and Numerical Methods

Because sustained microgravity cannot be replicated in terrestrial laboratories without free fall, experimental sloshing research relies on suborbital and orbital tests offering varying durations and microgravity qualities [5, 23, 24, 54, 55]. Levine et al. [40] and Liu et al. [56] utilized drop-tower platforms to measure surface tension, dynamic contact angles, and vane PMD liquid distribution. Parabolic flight aircraft (such as the ESA Airbus A310 ZERO-G and NASA KC-135) provide 20 to 25 seconds of reduced gravity per parabola across dozens of repeated maneuvers, enabling larger-scale test articles [5, 25, 26]. Storey and Kirk [25] and Storey et al. [27] conducted extensive parabolic flight campaigns characterizing spherical tank slosh dynamics using water and liquid nitrogen, while Arndt et al. [26] performed cryogenic sloshing tests in pressurized cylindrical vessels. The motivation is driven by the development of the new cryogenic upper stage of the European space Launcher (Ariane 5) as shown in Figure 2.7.

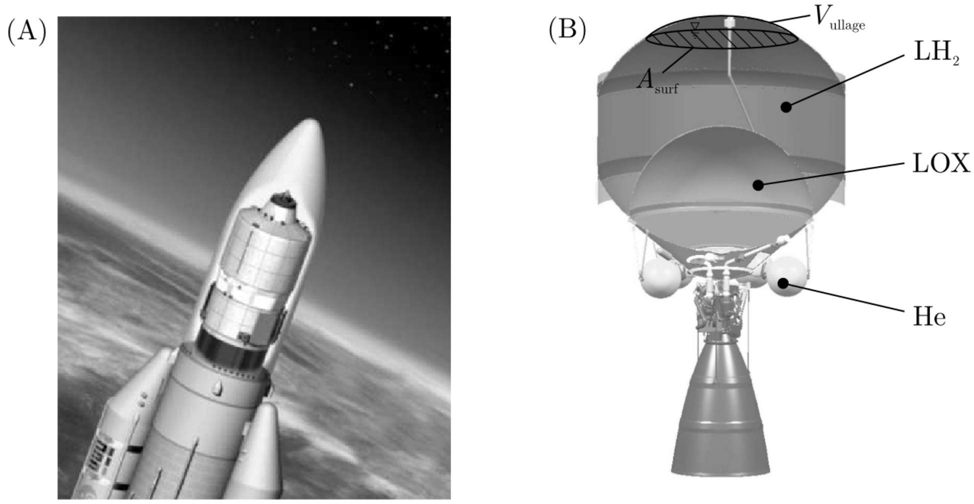

Figure 2.7. A) Ariane 5 Space Launcher B) Criogenic Upper Stage [26]

For long-duration investigations, orbital platforms eliminate the time constraints of parabolic flights [23, 54, 55]. The dedicated SloshSat-FLEVO mini-satellite, launched by ESA in 2005, carried an instrumented 87-liter tank containing 33.5 liters of water to study nonlinear fluid dynamics and GNC interaction in orbit [54, 57]. On the International Space Station, the SPHERES-Slosh experiment utilized free-floating automated satellites to gather long-duration slosh datasets for CFD benchmarking during robotic maneuvers [23, 55]. Ground-based hexapod and shake-table platforms complement flight experiments by evaluating large-scale tanks (such as 1,750-liter liquid hydrogen tanks investigated by Moran et al. [28]) and multi-axis sloshing platforms developed by Zhou et al. [24]. Luppes et al. [29] carried out experiments with the satellite 'Sloshsat FLEVO' shown in Figure 2.8.

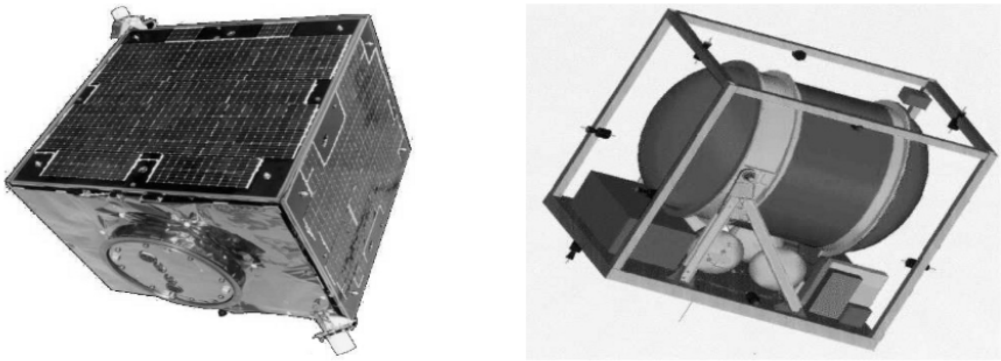

Figure 2.8. 'Sloshsat FLEVO' satellite [29]

Before 20th century, fluid motion was described analytically with Navier-Stokes (NS) and Euler equations, setting the base for later numerical methods. From its introduction in late 1950s till today, computational fluid dynamics (CFD) and finite element analysis (FEA) problems are mostly solved by discretization of a domain into a grid of connected elements (mesh). There are various mesh based numerical methods, such as finite difference method (FDM), finite volume method (FVM), finite element method (FEM), discontinuous Galerkin (DG), boundary element (BEM), Lattice Boltzmann (LBM), and spectral element method (SEM). FVM calculates the fluxes across the each cell faces using conservative equations. It is the most used method in industrial CFD, because of its proven reliability on complex geometry calculations and good coupling with turbulence models. FEM converts a partial differential equation from its classical form into an integral equation using test functions, and the application of Green's Theorem makes the implementation of numerical solution more efficient. Structured meshes can be computationally expensive to generate and maintain since they are approximating solutions using network of nodes distributed in the problem domain. In the past years, computing technology improvements, high order interpolation, and kernel-based methods have increased the interest in meshless methods, especially for complex multiphase flows and unsteady problems. [26–33]

As a Lagrangian, meshfree alternative to grid-based VOF methods, Smoothed Particle Hydrodynamics (SPH) has emerged as a powerful numerical framework for simulating violent sloshing, wave breaking, and fluid–structure interaction [34–36, 58]. In SPH, the fluid continuum is discretized into moving interpolation particles carrying mass, momentum, and energy, with field variables approximated through kernel interpolation functions $W(\mathbf{r} - \mathbf{r}', h)$:

$$f(\mathbf{r}) \approx \sum_b \frac{m_b}{\rho_b} f_b W(\mathbf{r} - \mathbf{r}_b, h) \tag{2.5}$$

Iglesias et al. [35] introduced SPH simulations for sloshing-type problems in anti-roll tanks, demonstrating that SPH naturally tracks severe free-surface fragmentation, splashing, and wall impacts without numerical diffusion or interface reconstruction errors. Bulian et al. [58] validated SPH for tuned liquid dampers with angular motion, while Arndt and Dreyer [34] established standardized experimental damping databases for cylindrical propellant vessels widely used as SPH validation benchmarks. Numerical methods summary is presented in Table 2.2.

Table 2.2. Numerical Methods Summary

Numerical Method	Discretization Framework	Free Surface Interface Tracking	Handling of Violent Splashing & Fragmentation	Computational Efficiency & Parallelization
Finite Volume Method (FVM)	Eulerian structured / unstructured mesh	Volume of Fluid (VOF) with geometric reconstruction	Moderate; prone to numerical diffusion and artificial droplet smearing	High on CPUs / GPUs; open-source solvers (OpenFOAM, Fluent)
Smoothed Particle Hydrodynamics (SPH)	Fully Lagrangian meshfree particles	Captured by particle positions;	Excellent; simulates droplet breakup and splashing	Highly parallelizable on GPUs
Moving Particle Semi-Implicit (MPS)	Lagrangian meshless particles (Incompressible pressure Poisson solver)	Implicit free surface tracking via particle number density	Excellent; accurately captures sharp impact pressures on tank baffles	Medium-High computational cost due to sparse Poisson equation solving
Lagrangian Differencing Dynamics (LDD)	Point cloud discretization based on Taylor series & Lanson-Vila scheme	Exact kinematic Lagrangian transport of moving point cloud	Excellent; high-order gradient accuracy without particle clustering instability	GPU-accelerated
Lattice Boltzmann Method (LBM)	Mesoscopic particle distribution functions on uniform lattice	Color-gradient or Shan-Chen multiphase pseudo-potential	Good for complex porous media (LAD screens); interface width can spread	Extremely fast and highly scalable on parallel GPUs

3. Passive Slosh Mitigation Technologies

3.1. Annular Ring Baffles

Internal mechanical baffles represent the standard approach to slosh mitigation in launch vehicle tanks. Flat annular ring baffles, mounted perpendicularly along the tank wall near the liquid surface, are the most common configuration [1, 59, 60]. Ibrahim et al. [3] address the means of passive control of propellant sloshing and vibratory structures control with sloshing forces in their review article. Miles [61] developed the classical analytical expression for the equivalent viscous damping ratio ζ provided by an annular ring baffle in a circular container:

$$\zeta = 2.83\, e^{-4.60d/R} \left(\frac{w}{R}\right)^{3/2} \left(\frac{\eta_0}{R}\right)^{1/2} \tag{3.1}$$

Here w is the baffle width, d is the liquid depth above the baffle, R is the tank radius, and η_0 is the wave amplitude at the wall. The Miles equation highlights three key relationships: damping decays exponentially as the liquid level departs from the baffle plane ($d/R > 0$), scales with baffle width as $(w/R)^{3/2}$, and increases with the square root of wave amplitude [61, 62]. NASA SP-803 [59] consolidated these relationships into standard design criteria for launch vehicles. Stephens and Leonard [63] and Chintalapati et al. [64] tested ring baffles (see Fig. 3.1) in spheroidal and cylindrical tanks, documenting the effects of baffle thickness, perforation ratio, and liquid depth on vortex shedding. To reduce weight, Brooks and Stephens [65] developed flexible ring baffles using thin elastomeric and composite materials (see Fig. 3.2). Their work showed that flexible baffles match or exceed rigid baffle damping through fluid–structure interaction while reducing half of the structural weight.

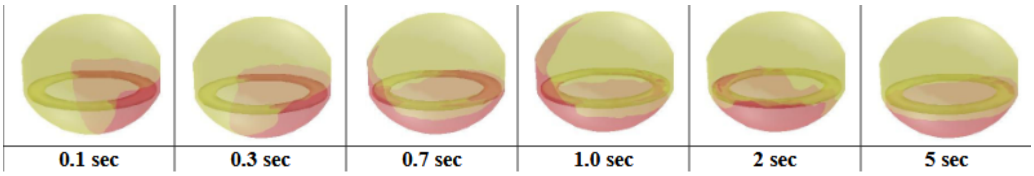

Figure 3.1. 3D Tank Flow With an Annular Slosh Baffle Inside [64]

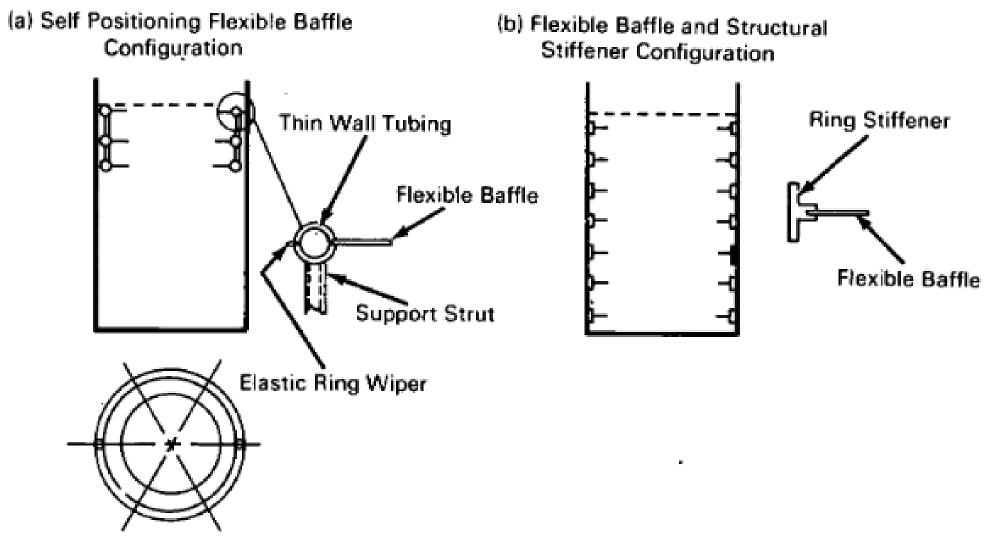

Figure 3.2. Flexible Baffle Configuration [65]

Wang et al. [66] used an analytical approach to study the sloshing natural frequencies and modes in a cylindrical container with annular baffle configuration (see Figure 3.3). The Fourier-Bessel expansion on the free surface and the artificial interfaces are used to obtain the Eigen-frequency equation. This method has shown high accuracy and small computational costs.

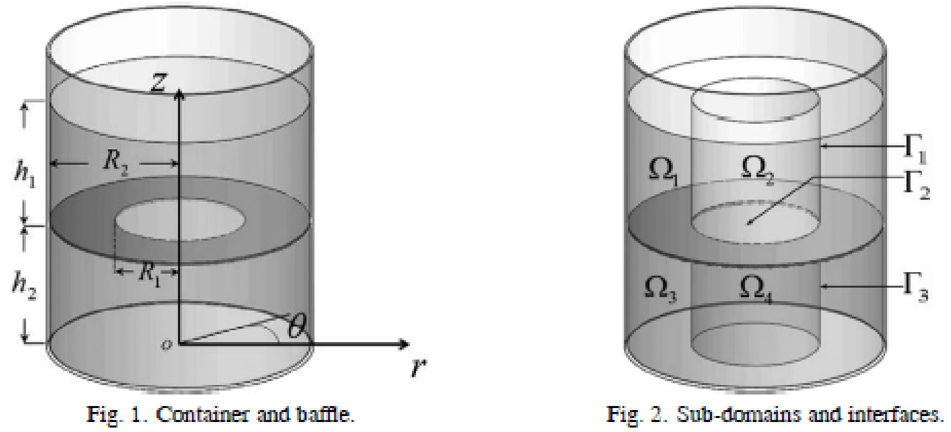

Figure 3.3. Annular Baffle Configuration [66]

3.2. Surface-Tension Propellant Management Devices (PMDs)

Propellant management devices (PMDs) are used to separate fluid and gas phases and transfer vapor-free propellant from a a storage tank to the next transfer line device (ex. engine, depot tank). Hartwig [17], following the foundational PMD design analyses by Jaekle [67, 68] and tank implementations studies [69, 70], analysed and compared the three primary capillary-driven propellant management device types of vanes, sponges, and screen channel liquid acquisition devices (see Figs. 3.3, 3.4 and 3.5). The author concluded that the vanes and sponges may not be the best choice for future devices. Vanes may not be able to supply large low rates and the sponges do not scale with the projected size of depot tanks, while screen channel LADs may provide a wide range of possibilities.

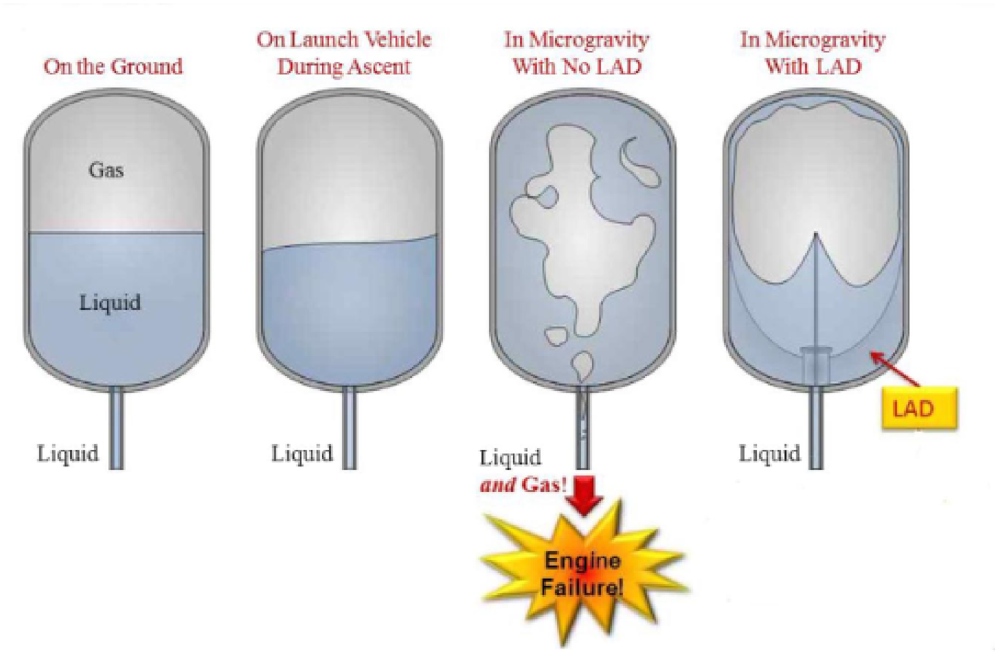

Figure 3.4. Scheme of why Liquid Acquisition Devices are Required [17]

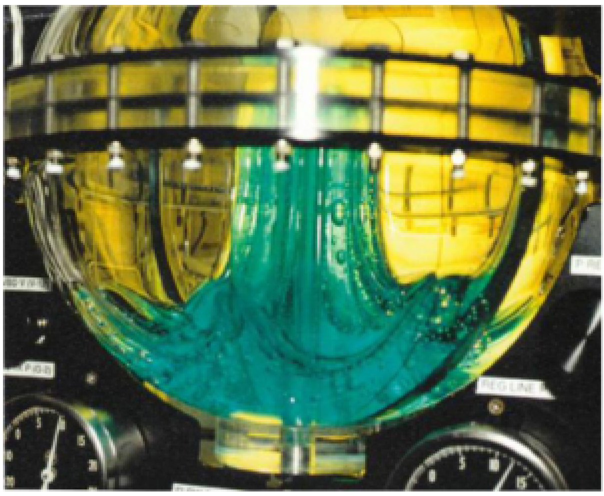

Figure 3.5. FARE-II Vane and Sponge [17]

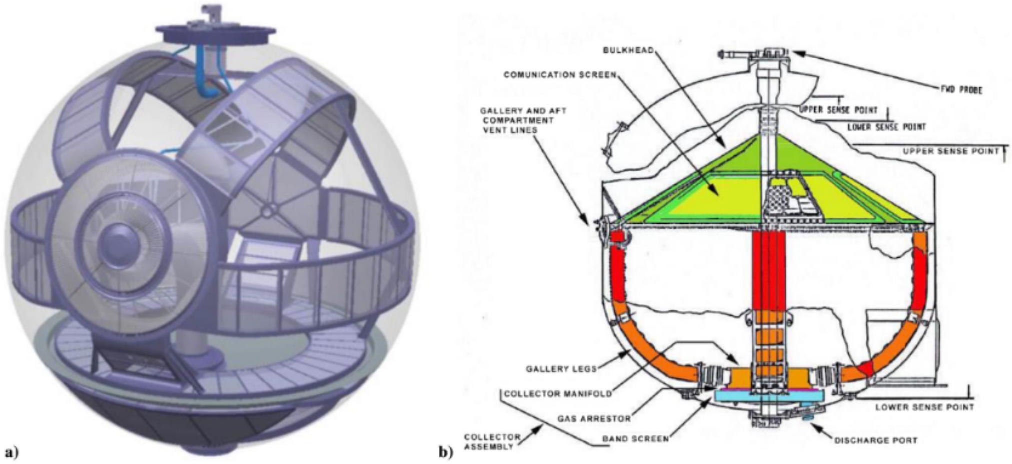

Figure 3.6. Screen Channel Liquid Acquisition Device (LAD) [17]

An LAD operates within the limit of its bubble-point pressure ΔP_{bp}:

$$\Delta P_{BP} = \frac{4\gamma \cos\theta_C}{D_{p,293K}} \tag{3.2}$$

where D_p is the effective pore diameter [71]. Vasireddy et al. [71] and Wang et al. [72] developed 3D transient flow models and screen-compliance experiments, showing that elastic screen deflection during flow startup affects flow distribution and bubble-point integrity. Weislogel et al. [73, 74] and McCraney et al. [75] reviewed experiments from the International Space Station and drop towers, showing that passive capillary structures reliably transport and separate multiphase fluids across large tank dimensions. Weislogel and Collicott [76] and Liu et al. [56, 77] used drop-tower tests and VOF simulations to analyse liquid distribution in vaned tanks under low gravity. He et al. [78] summarize the research progress on liquid directional transport surfaces that guide liquid movement along tank walls, providing design guidelines for passive fluid control (see Figure 3.6).

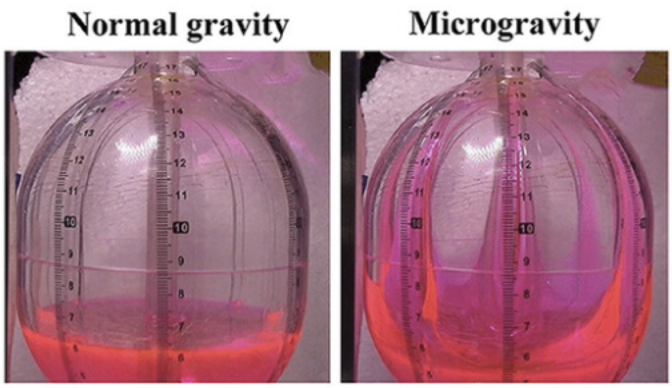

Figure 3.7. Liquid movement along tank walls [78]

3.3. Tuned Liquid Dampers (TLDs)

Tuned Liquid Damper (TLD) and Tuned Liquid Column Damper (TLCD) are passive control concepts widely used in civil engineering and construction. A TLD consists of a attached fluid filled tank on a vibrating structure, tuned so that its sloshing frequency matches the natural frequency of the structure. There is growing interest in TLDs due to their low maintenance costs and ease of installation [58, 79]. Bulian et al. [58] developed Smoothed Particle Hydrodynamics (SPH) simulations of TLDs for single degree of freedom system. Konar et al [79] provided an overview of real implementations of TLD and flow damping devices (FDD) in various structures (see Figs. 3.7 and 3.8). It highlights the other less explored options which can be used in TLDs, such as sand, submerged particles, floating baffles, etc.

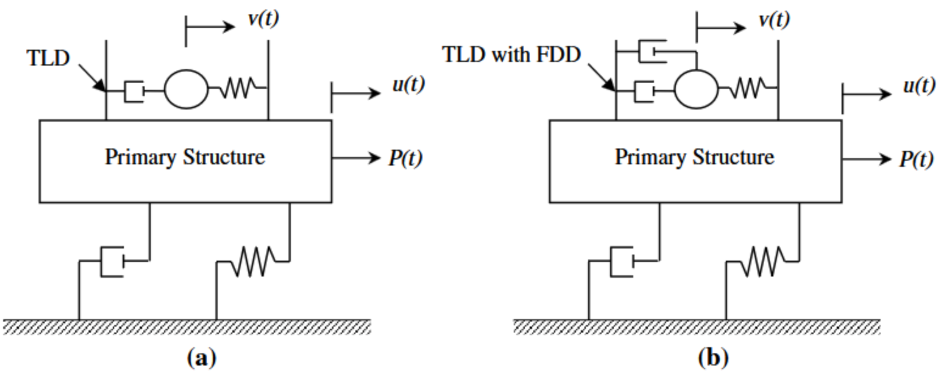

Figure 3.8. a) Primary structure-TLD, b) Primary structure-TLD with FDD [79]

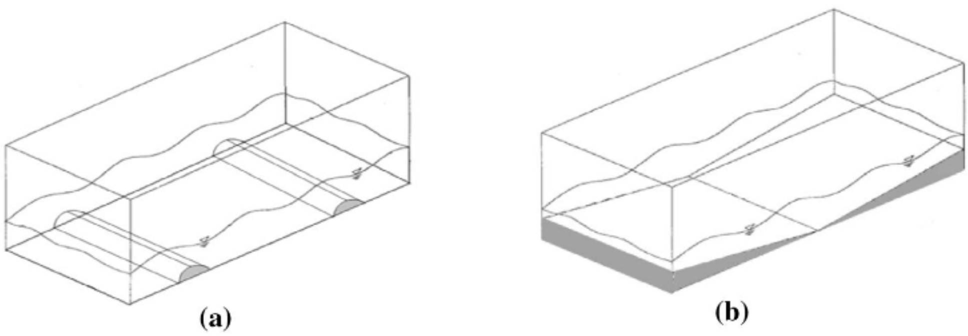

Figure 3.9. a) TLD-Curved Obstacles, b) TLD-Wedge Type Obstacles [79]

3.4. Summary Table

Based on reviewed literature, passive sloshing devices summary is presented in Table 3.1.

Table 3.1. Summary of Passive Sloshing Control Devices

Passive Control	Working Principle	Structure Mass	Spaceflight Use	Limitations
Rigid Annular Ring Baffles	Vortex appears and viscous dissipation at sharp baffle edges	High (adds 50–200 kg per stage in metal structures)	High (TRL 9: Apollo, Saturn V, Ariane, Centaur)	Fixed spatial location; ineffective when liquid surface departs from baffle plane
Flexible Baffles	Fluid-Structure Interaction (FSI); elastic deformation increase energy dissipation	Medium (up to 50% mass reduction vs. rigid baffles)	Medium (TRL 5–6: Sounding rockets, ground tests)	Material fatigue, cryogenic compatibility limited
PMD: Vanes and Sponges	Surface-tension capillary pumping along narrow gaps and intersecting corners	Low to Medium (Lightweight metal vanes)	High (TRL 9: Geostationary communication satellites)	Limited maximum flow rate capacity; does not scale to large depot tanks
Screen Channel LADs	Bubble-point surface tension barrier: preventing vapor ingestion	Low (Titanium/stainless steel fine mesh channels)	High (TRL 8–9: Cryogenic upper stages, orbital transfer vehicles)	Screen compliance deflection, breakdown under high dynamic surge pressures
Tuned Liquid Dampers (TLDs / TLCDs)	Liquid sloshing resonance in auxiliary tank dissipates host structure energy	Medium (Tank and fluid mass required)	High in civil structures; Low (TRL 3–4) in spacecraft	Frequency-sensitive; detuning occurs under varying liquid levels and accelerations
Directional Transport Surfaces	Micro-grooved and gradient-wettability surface patterns guide liquid film migration	Very Low (Surface coating)	Low (TRL 3–4: Laboratory and drop tower tests)	Sensitive to surface contamination, coating degradation and thermal impact

4. Active Sloshing Control

4.1. Active Damping

Passive baffles disadvantages, such as fixed frequency and reduced effectiveness for different filling levels, have emerged interest in active slosh control. The most advanced mechanical approach uses force-feedback control of the tank mounting structure, developed by Konopka et al. [18] and Jetzschmann et al. [80]. Konopka et al. [18] investigated first mode water sloshing in a 1.2 m diameter Perspex tank mounted abroad the DLR Hexapod system. The final phase simulator (FiPS) simulations of sloshing experiments showed that the experimental forces are matched withing 5% uncertainty. Jetzschmann et al. [80] illustrated that is possible to actively control sloshing via closed loop by using force feedback for the slosh resonance compensation.

4.2. Mobile Baffles and PMD Membranes

In active PMD design there are two concepts: electromagnetic membranes and acoustic membranes. Gligor et al. [81] and Tang et al. [82] studied mobile baffles that translate or rotate via electromagnetic or mechanical actuators. By tracking the liquid free surface, mobile baffles maintain optimal immersion depth and damping across all fill levels. Gligor et al. [81] studied sloshing control with moving baffles constrained by springs drawing the idea from TMDs success. It highlights the need for further researches on various extensions of these systems for different filling ratios. Figure 4.1 shows the results for fixed and moving baffle effects on a fluid system, and the flow with maximum deformation of the fluid surface for the moving baffle case.

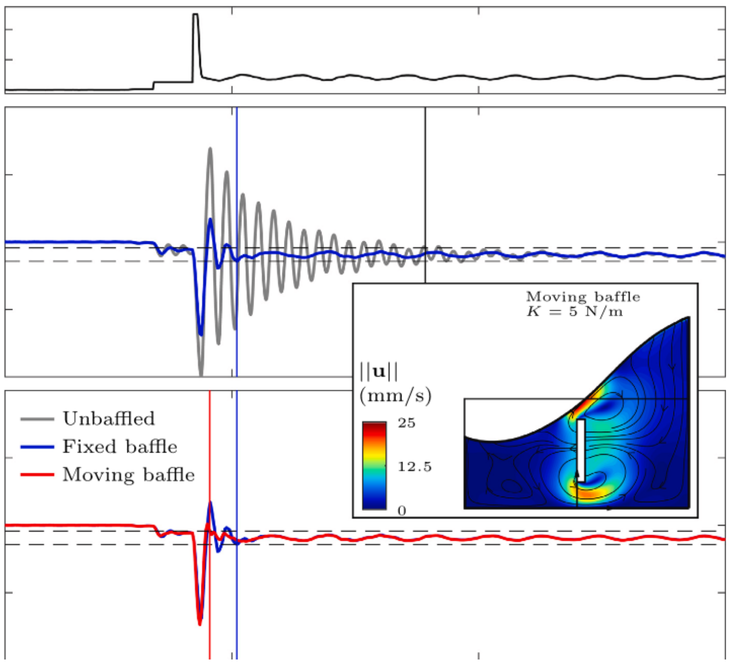

Figure 4.1. Fixed and Moving Baffle Effects on a Fluid System [81]

Alvaro et al. [83] preliminary results in ferrofluid dynamics in microgravity conditions point to significant contributions. Using an optical surface reconstruction tool, they tested ferrofluid sloshing under magnetic fields, measuring lateral and axisymmetric natural frequencies and damping ratios [83–88]. They measured magnetic forces on ferrofluid droplets, verified magnetic slosh dispersion equations and developed the Magnetic Positive Positioning (MP2) concept for propellant settling prior to engine restart. Hart et al. [89] extended the approach to thermo-electromagnetic SmallSat propellant management using localized cooling and magnetic coils. However, magnetic slosh control faces two fundamental physical constraints: magnetic fields decay rapidly with distance, limiting their reach in large tanks, and doping propellants with solid nanoparticles risks chemical degradation and engine fouling. Authors in this field note that non-magnetic active methods, particularly acoustic and vibroacoustic actuation, remain unexplored in the microgravity sloshing literature.

4.3. Piezoelectric Actuation

Qi et al. [90] studied an embedded piezoelectric actuator with a sandwich configuration for active vibration control as shown in Figure 4.2. The vibration control and the method correctness were verified by simulation and experiment. The actuator shows strong advantages in vibration control at low frequencies and has a good perspective in the aerospace application.

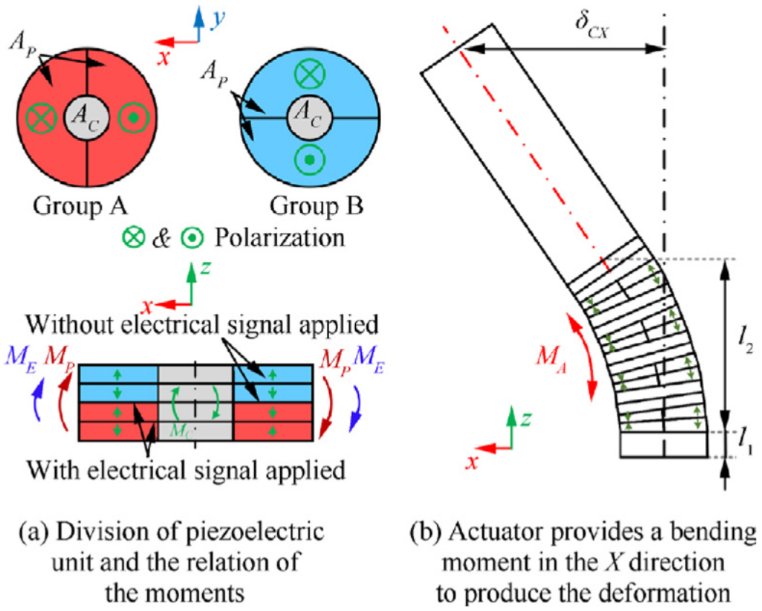

Figure 4.2. Piezoelectric actuator [90]

4.4. Attitude Control

Hervas et al. [91] expressed the equations of motion in terms of 3D spacecraft translational velocity vector, the attitude and angular velocity, and the internal coordinates. Studies [57, 92–98] analysed physical disturbance, active suppression and alternative control strategies to mitigate sloshing induced spacecraft disturbances. Leiter et al. [96] presented robust spacecraft attitude control of SpaceIL's lunar lander Beresheet (see Fig. 4.3) under multi tank sloshing disturbances.

The methodology proved successful in 10 orbit correction maneuvers.

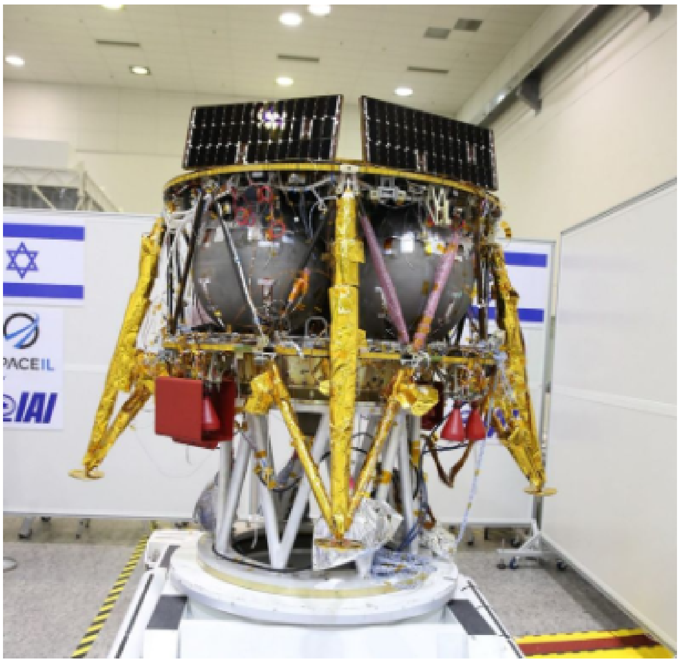

Figure 4.3. SpaceIL's lunar lander Beresheet [96]

4.5. Summary Table

Based on reviewed literature, active sloshing devices summary is presented in Table 4.1.

Table 4.1. Summary of Active Sloshing Control Devices

Active Control	Working Principle	Structure Mass	Limitations
Force Structural Control (Hexapod)	Multi-axis active suspension adjusts tank orientation based on force sensor feedback	High mass: hydraulic/electric hexapod actuators	Adds complex external structural mechanisms
Translating Baffles	Electromechanical or spring-constrained moving baffles track moving liquid interface	Lower mass than hexapods: internal track actuators	Seal wear, jamming, and cryogenic freeze-up
Magnetic Positive Positioning	Magnetic field gradients generate Kelvin body force on ferrofluid propellants	Electrical coil mass: high instantaneous power	Nanoparticle agglomeration, magnetic weakening over large distances
Piezoelectric Transducers	High-frequency structural acoustic vibration and localized wall excitation	Low mass: compact piezoelectric patches	High voltage amplification requirements
Attitude Control	Thruster and reaction wheel control laws feedforward-cancel slosh wave motion	No mass: software/GNC algorithm	Sensitive to parameter uncertainty; ineffective during extreme slosh transitions
Acoustic Radiation Control (Proposed)	Ultrasonic phased arrays exert directed acoustic radiation force on liquid interface	Low mass:solid-state transducer arrays	High acoustic damping at high frequencies; nonlinear streaming and thermal energy loss

5. Vibroacoustic in Fluid Systems

5.1. Faraday Waves

Faraday waves appear at the surface of the liquid inside of the tank subjected to vertical excitation. Faraday threshold is a critical driving acceleration above which the entire free surface becomes unstable to a standing field of waves [99]. The uniform Faraday pattern (see Fig. 5.1) becomes chaotic when the driving acceleration is increased to a secondary order-disorders instability. Traveling Faraday waves may also move along channels with variable curvature and more complex geometries.

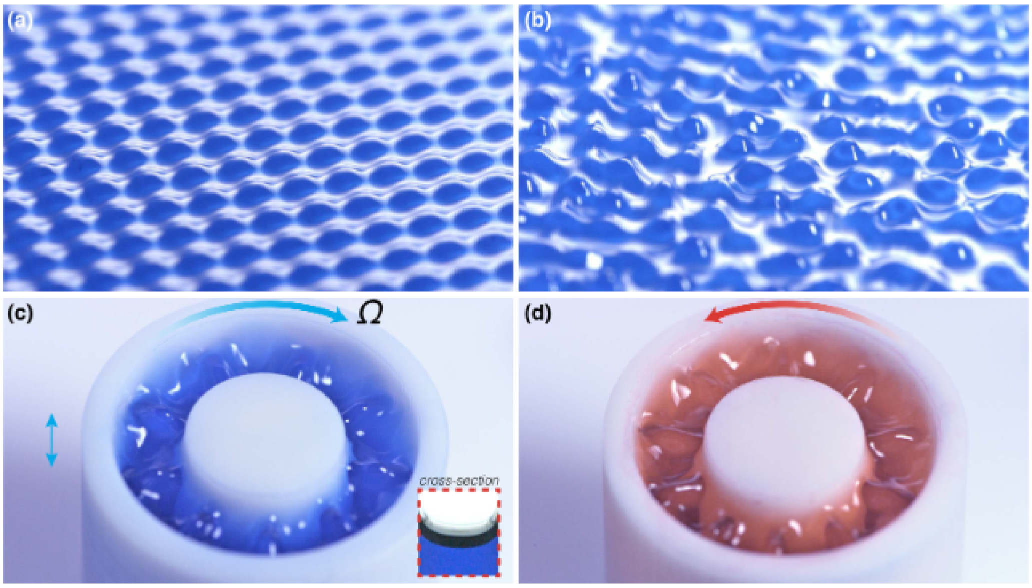

Figure 5.1. Symmetry-braking of Faraday waves. a) Standing Surface Waves b) Chaotic Faraday Pattern c-d) Faraday Waves in Annular channel c) clockwise and d) counterclockwise [99]

In propellant tanks, parametric vibration can cause dangerous slosh resonance [100–103]. Colville et al. [102] and López et al. [101] investigated horizontal cylindrical tanks under forced harmonic and parametric excitation, identifying distinct sloshing regimes, wave breaking limits, and wall load distributions (see Fig. 5.2). López et al. [101] identified two resonant frequencies as governing the behaviour of the liquid free surface. Experimental results matched closely the theoretical predictions of the two antisymmetric sloshing modes. Roux et al. [104] demonstrated the effect of layers of polystyrene beads placed on the surface of isopropanol undergoing a low frequency vertical sinusoidal excitation. The results show that a sufficient number of beady is needed to prevent Faraday waves.

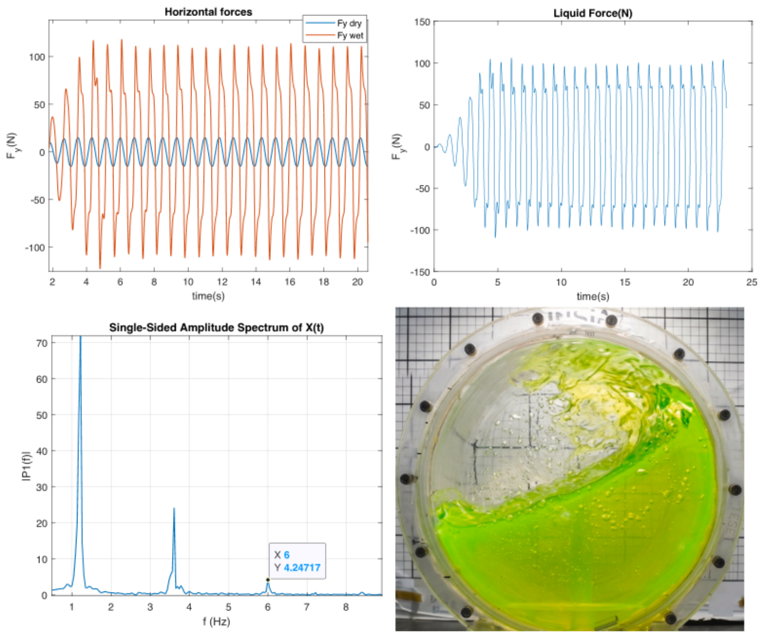

Figure 5.2. Fast Fourier Transform of the Wet Force Signal and the Snapshot of a Typical Impact [101]

5.2. Structural Vibroacoustics

Structural vibroacoustics studies how vibrating plates, shells, and hull structures radiate sound into surrounding fluids. The vibroacoustic excitations are mainly due to noise generated by the launcher during ignition, atmospheric flight or lift off. Ibrahim [105] reviewed recent advances in vibro-impact dynamics, structural collisions, and acoustic radiation damping for ocean and aerospace structures. Its primary goal is reducing structure noise or vibration. Study by Issal et al. [106] gives an insight into the structural-acoustic response of a lightweight square aluminium panel (see Fig. 5.3). Both, experimental and numerical measurements were used and validated. Various positions of the sound source were analysed and concluded that the position of the sound source significantly affects the panel's vibro-acoustic reduction performance. With the resulting characteristics the optimal placement was determined for active noise control.

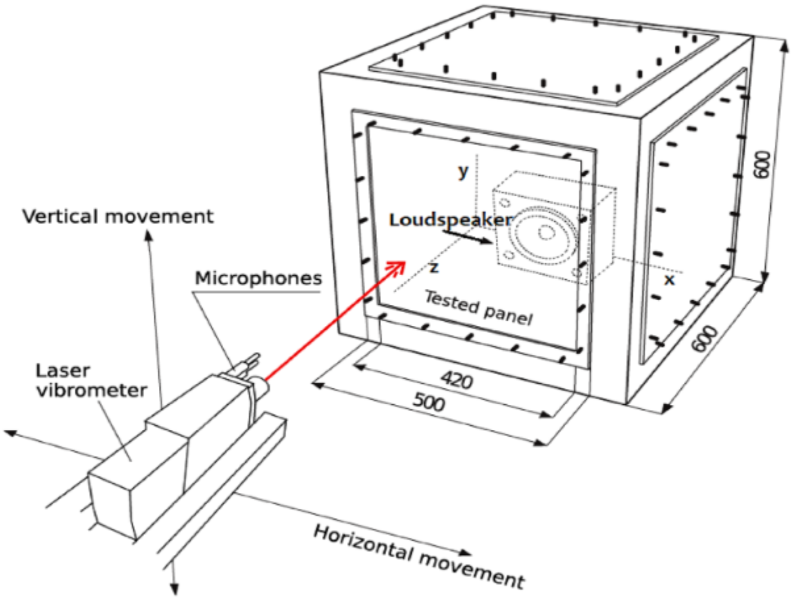

Figure 5.3. Experimental Setup Scheme for acoustic radiation measurements [106]

Lukovsky and Timokha [107] brought theoretical study of acoustic interaction affecting the dynamics and stability of limited fluid volume in microgravity conditions. They proved that standing acoustic fields can induce stabilization and destabilization of capillary interfaces, formulating the concept of Capillary acoustic equilibria. Their findings provide theoretical confirmation that acoustic radiation pressure can act as an effective governing force on liquid interfaces in microgravity environments, providing the physical basis for active acoustic slosh control.

6. Conclusion

Reviewing the literature in Sections 2 through 5 there are several key gaps in microgravity propellant slosh control noticed. Fixed ring baffles and PMDs remain the industry standard but due to heavy structural mass (up to 200 kg per vehicle), lose effectiveness away from nominal fill levels, and cannot adapt during flight. Although existing active systems showed improvement compared to passive systems, there are still some major issues. Mechanical hexapods add heavy actuators and moving structural parts, while magnetic ferrofluid positioning in large tanks fails due to magnetic properties loss with distance. In contrast, acoustic waves propagate through any liquid supporting pressure waves (LOX, LH_2, LCH_4, hydrazine, water) without chemical additives or nanoparticle doping. Also, acoustic energy can be directed and focused across a tank volume using piezoelectric phased arrays.

Although acoustic radiation pressure has been investigated from early NASA phased-array studies to recent cryogenic ullage-trapping programs, existing works focuses mostly on localized fluid management. The primary scientific gap is the absence of a validated framework for using high-frequency acoustic radiation pressure to actively suppress global, low-frequency capillary sloshing modes at tank scale.

To address these gaps, the proposed doctoral research investigates acoustic slosh control in microgravity conditions. The research is implementing acoustic source terms into multiphase CFD (VOF) and Lagrangian particle methods to model interface stabilization and damping under microgravity. Comparing acoustic control against passive baffles and magnetic systems in terms of damping ratio, power consumption, response time, and mass savings. This research should unite computational fluid dynamics (RANS/VOF), structural finite element dynamics, and meshless modelling in Python to develop an active fluid control methodology for space applications.

References

[1] Abramson, H. N.: “The Dynamic Behavior of Liquids in Moving Containers”, NASA SP-106, 1966.

[2] Ibrahim, R. A.: “Liquid Sloshing Dynamics: Theory and Applications”, Cambridge University Press, 2005. https://doi.org/10.1017/CBO9780511536656

[3] Ibrahim, R. A.; Pilipchuk, V. N.; Ikeda, T.: “Recent Advances in Liquid Sloshing Dynamics”, Applied Mechanics Reviews, Vol. 54, No. 2, pp. 133-199, 2001. https://doi.org/10.1115/1.3097293

[4] Peterson, L. D.; Crawley, E. F.: “Nonlinear fluid slosh coupled to the dynamics of a spacecraft”, AIAA Journal, Vol. 26, No. 8, pp. 975–982, 1988. https://doi.org/10.2514/3.10001

[5] Simonini, A.; Dreyer, M.; Urbano, A. et al.: “Cryogenic propellant management in space: open challenges and perspectives”, npj Microgravity, Vol. 10, Art. no. 34, 2024. https://doi.org/10.1038/s41526-024-00377-5

[6] Dodge, F. T.; Garza, L. R.: “Experimental and theoretical studies of liquid sloshing at simulated low gravity”, Journal of Applied Mechanics, Vol. 34, No. 3, pp. 555-562, 1967. https://doi.org/10.1115/1.3607746

[7] Dodge, F. T.; Garza, L. R.: “Simulated low-gravity sloshing in spherical, ellipsoidal, and cylindrical tanks”, Journal of Spacecraft and Rockets, Vol. 7, No. 2, pp. 204-206, 1970. https://doi.org/10.2514/3.29906

[8] Dodge, F. T.; Garza, L. R.: “Simulated low-gravity sloshing in spherical tanks and cylindrical tanks with inverted ellipsoidal bottoms”, Southwest Research Institute Technical Report No. 2, SwRI Project 02-2342, 1972.

[9] Cassoni, G.: “Curvature-corrected sloshing spectra for cylindrical tanks in microgravity”, arXiv preprint arXiv:2605.00168, Roma Tre University, 2026. https://doi.org/10.48550/arXiv.2605.00168

[10] Utsumi, M.: “The meniscus and sloshing of a liquid in an axisymmetric container at low-gravity”, JSME International Journal Series C, Vol. 33, No. 3, pp. 346-356, 1990. https://doi.org/10.1299/jsmec1988.33.346

[11] Concus, P.; Finn, R.: “On the behavior of a capillary surface in a wedge”, Proceedings of the National Academy of Sciences of the United States of America, Vol. 63, No. 2, pp. 292-299, 1969. https://doi.org/10.1073/pnas.63.2.292

[12] Dalmon, A.; Lepilliez, M.; Tanguy, S. et al.: “Comparison Between the FLUIDICS Experiment and Direct Numerical Simulations of Fluid Sloshing in Spherical Tanks Under Microgravity Conditions”, Microgravity Science and Technology, Vol. 31, No. 2, pp. 123-138, 2019.

https://doi.org/10.1007/s12217-019-9675-4

[13] Li, D.; Lin, J.: "Dynamic behavior in a storage tank in reduced gravity using dynamic contact angle method", Microgravity Science and Technology, Vol. 32, pp. 883-894, 2020. https://doi.org/10.1007/s12217-020-09831-x

[14] Anderson, E. Z.; Chintalapati, S.; Kirk, D.: "Modeling of ullage collapse within rocket propellant tanks at reduced gravity", Journal of Spacecraft and Rockets, Vol. 51, No. 5, pp. 1377-1389, 2014. https://doi.org/10.2514/1.A32308

[15] Abramson, H. N.; Chu, W.-H.; Garza, L. R.: "Liquid sloshing in spherical tanks", AIAA Journal, Vol. 1, No. 2, pp. 384–389, 1963. https://doi.org/10.2514/3.1542

[16] Wang, L. et al.: "Numerical Simulation of the Reorientation Process Under Different Conditions in a Vane-type Surface Tension Propellant Tank", Microgravity Science and Technology, Vol. 34, Art. no. 73, 2022. https://doi.org/10.1007/s12217-022-09950-7

[17] Hartwig, J. W.: "Propellant management devices for low-gravity fluid management: past, present, and future applications", Journal of Spacecraft and Rockets, Vol. 54, No. 4, pp. 808-824, 2017. https://doi.org/10.2514/1.A33750

[18] Konopka, M.; De Rose, F.; Strauch, H.; Jetzschmann, C.; Darkow, N.; Gerstmann, J.: "Active slosh control and damping-Simulation and experiment", Acta Astronautica, Vol. 158, pp. 89-102, 2019. https://doi.org/10.1016/j.actaastro.2018.06.055

[19] Romero-Calvo, Á.; Maggi, F.; Schaub, H.: "Magnetic positive positioning: Toward the application in space propulsion", Acta Astronautica, Vol. 187, pp. 348-361, 2021. https://doi.org/10.1016/j.actaastro.2021.06.045

[20] Reyhanoglu, M.: "Modelling and control of space vehicles with fuel slosh dynamics", in Advances in Spacecraft Technologies, J. Hall (Ed.), InTech, pp. 441-460, 2011. ISBN: 978-953-307-551-8.

[21] Fisher, M. F.; Schmidt, G. R.; Martin, J. J.: "Analysis of cryogenic propellant behaviour in microgravity and low thrust environments", Cryogenics, Vol. 32, No. 2, pp. 230-235, 1992. https://doi.org/10.1016/0011-2275(92)90272-C

[22] Werner, M. P. et al.: "Ballistic Phase Performance Model for Cold Gas Attitude Control in Cryogenic Upper Stages", in 51st AIAA/SAE/ASEE Joint Propulsion Conference, AIAA 2015-3814, 2015. https://doi.org/10.2514/6.2015-3814

[23] Chintalapati, S. et al.: "Design of an experimental platform for acquisition of liquid slosh data aboard the International Space Station", in 50th AIAA Aerospace Sciences Meeting, AIAA 2012-4297, 2012. https://doi.org/10.2514/6.2012-4297

[24] Zhou, R. et al.: "Experimental and Numerical Investigation of Liquid Slosh Behavior Using Ground-Based Platforms", Journal of Spacecraft and Rockets, Vol. 49, No. 5, pp. 917-929,

2012. https://doi.org/10.2514/1.A32052

[25] Storey, J. M.; Kirk, D. R.: "Experimental Investigation of Spherical Tank Slosh Dynamics with Water and Liquid Nitrogen", Journal of Spacecraft and Rockets, Vol. 57, No. 4, pp. 783-795, 2020. https://doi.org/10.2514/1.A34471

[26] Arndt, T. et al.: "Cryogenic Sloshing Tests in a Pressurized Cylindrical Reservoir", in 45th AIAA/ASME/SAE/ASEE Joint Propulsion Conference & Exhibit, AIAA 2009-4860, 2009. https://doi.org/10.2514/6.2009-4860

[27] Storey, J. et al.: "Experimental, Numerical and Analytical Characterization of Slosh Dynamics Applied to In-Space Propellant Storage and Management", in AIAA Space 2015 Conference and Exposition, AIAA 2015-4077, 2015. https://doi.org/10.2514/6.2015-4077

[28] Moran, M. et al.: "Experimental results of hydrogen slosh in a 62 cubic foot (1750 liter) tank", NASA Technical Memorandum TM-106506, 1994.

[29] Luppes, R.; Helder, J. A.; Veldman, A. E. P.: "The Numerical Simulation of Liquid Sloshing in Microgravity", in European Conference on Computational Fluid Dynamics (ECCOMAS CFD 2006), P. Wesseling, E. Onate, J. Périaux (Eds.), Delft, The Netherlands, 2006. https://doi.org/10.1007/978-3-540-92779-2_95

[30] Veldman, A. E. P.; Gerrits, J.; Luppes, R.; Helder, J. A.; Vreeburg, J. P. B.: "The numerical simulation of liquid sloshing on board spacecraft", Journal of Computational Physics, Vol. 224, No. 1, pp. 82-99, 2007. https://doi.org/10.1016/j.jcp.2006.12.020

[31] Lu, Z.; Cao, Z.; Xia, Z.; Zhang, X.; Yuan, X.: "Numerical simulation and optimization study of liquid sloshing in a LNG storage tank", Journal of Marine Science and Engineering, Vol. 14, No. 6, p. 525, 2026. https://doi.org/10.3390/jmse14060525

[32] Hung, R. J. et al.: "Sloshing of cryogenic helium driven by lateral impulse/gravity gradient-dominated/or g-jitter-dominated accelerations and orbital dynamics", Cryogenics, Vol. 36, No. 12, pp. 1007-1018, 1996. https://doi.org/10.1016/0011-2275(96)00046-X

[33] Himeno, T. et al.: "Investigation on heat exchange enhanced by sloshing", in 44th AIAA/ASME/SAE/ASEE Joint Propulsion Conference & Exhibit, AIAA 2008-4550, 2008. https://doi.org/10.2514/6.2008-4550

[34] Arndt, T. O.; Dreyer, M. E.: "Damping behavior of sloshing liquid in laterally excited cylindrical propellant vessels", Journal of Spacecraft and Rockets, Vol. 45, No. 5, pp. 1085-1091, 2008. https://doi.org/10.2514/1.37050

[35] Souto-Iglesias, A.; Pérez-Rojas, L.; Zamora-Rodríguez, R.: "Simulation of anti-roll tanks and sloshing type problems with smoothed particle hydrodynamics", Ocean Engineering, Vol. 31, No. 8-9, pp. 1169-1192, 2004. https://doi.org/10.1016/j.oceaneng.2003.09.002

[36] Kotsarinis, K. et al.: "Modeling sloshing damping for spacecraft: A smoothed particle hydrodynamics application", Aerospace Science and Technology, Vol. 135, p. 108090, 2023. https://doi.org/10.1016/j.ast.2022.108090

[37] Bašić, J.; Blagojević, B.; Andrun, M.; Degiuli, N.: "A Lagrangian Finite Difference Method for Sloshing: Simulations and Comparison with Experiments", in Proceedings of the 29th International Ocean and Polar Engineering Conference (ISOPE), Sapporo, Japan, pp. 2095-2102, 2019.

[38] Lanson, N.; Vila, J.: "Renormalized meshfree schemes I: consistency, stability, and hybrid methods for conservation laws", SIAM Journal on Numerical Analysis, Vol. 46, No. 4, pp. 1912-1934, 2008. https://doi.org/10.1137/S0036142903427718

[39] Jang, J.; Alaniz, A.: "Mechanical slosh models for rocket-propelled spacecraft", in AIAA Guidance, Navigation, and Control Conference, AIAA 2013-4651, 2013. https://doi.org/10.2514/6.2013-4651

[40] Levine, D.; Wise, B.; Schulman, R. et al.: "Surface tension and contact angle analysis with design of propellant measurement apparatus", Journal of Propulsion and Power, Vol. 31, No. 2, pp. 429-439, 2015. https://doi.org/10.2514/1.B35213

[41] Utsumi, M.: "Slosh damping caused by friction work due to contact angle hysteresis", AIAA Journal, Vol. 55, No. 1, pp. 265-273, 2017. https://doi.org/10.2514/1.J055238

[42] Capolupo, F.: "Equivalent mechanical models for sloshing", arXiv preprint arXiv:2511.10172, 2025. https://doi.org/10.48550/arXiv.2511.10172

[43] Graham, E. W.: "The forces produced by fuel oscillation in a rectangular tank", Douglas Aircraft Company Report No. SM-13748, Santa Monica, CA, 1951.

[44] Graham, E. W.; Rodriquez, A. M.: "The characteristics of fuel motion which affect airplane dynamics", Journal of Applied Mechanics, Vol. 19, No. 3, pp. 381-388, 1952. https://doi.org/10.1115/1.4010515

[45] Utsumi, M.: "Low-gravity sloshing in an axisymmetrical container excited in the axial direction", Journal of Applied Mechanics, Vol. 71, No. 5, pp. 642-650, 2004. https://doi.org/10.1115/1.1307500

[46] Utsumi, M.: "A mechanical model for low-gravity sloshing in an axisymmetric tank", Journal of Applied Mechanics, Vol. 71, No. 5, pp. 651-659, 2004. https://doi.org/10.1115/1.1794700

[47] Utsumi, M.: "Slosh Analysis for Teardrop Tank", Journal of Spacecraft and Rockets, Vol. 45, No. 5, pp. 1007-1014, 2008. https://doi.org/10.2514/1.35156

[48] Gao, T. et al.: "Modeling Torsional Stiffness and Damping of Liquid Slosh in Spacecraft Diaphragm Tanks", Journal of Spacecraft and Rockets, Vol. 61, No. 3, pp. 883-894, 2024. https://doi.org/10.2514/1.A36019

[49] Kana, D. D.: "A Model for Nonlinear Rotary Slosh in Propellant Tanks", Journal of Spacecraft and Rockets, Vol. 24, No. 2, pp. 169-177, 1987. https://doi.org/10.2514/3.25891

[50] Farid, M.; Gendelman, O. V.: "Internal resonances and dynamic responses in equivalent mechanical model of partially liquid-filled vessel", Journal of Sound and Vibration, Vol. 379, pp. 191–212, 2016. https://doi.org/10.1016/j.jsv.2016.05.046

[51] Miao, N.; Yue, B. Z.: "Equivalent mechanical model of large-amplitude liquid sloshing", Journal of Sound and Vibration, Vol. 390, pp. 147-163, 2017. https://doi.org/10.1016/j.jsv.2016.08.029

[52] Miao, N. et al.: "Large-amplitude sloshing analysis and equivalent mechanical modeling in spherical tanks of spacecraft", Journal of Spacecraft and Rockets, Vol. 53, No. 6, pp. 1168-1178, 2016. https://doi.org/10.2514/1.A33394

[53] Yang, H. Q.; Peugeot, J. W.: "Propellant sloshing parameter extraction from computational-fluid-dynamics analysis", Journal of Spacecraft and Rockets, Vol. 51, No. 6, pp. 1827-1836, 2014. https://doi.org/10.2514/1.A32608

[54] Prins, J.: "SLOSHSAT FLEVO facility for liquid experimentation and verification in orbit: description of the mini satellite", National Aerospace Laboratory NLR Report NLR-TP-2000-025, 2000.

[55] Lapilli, G. D.; Kirk, D.; Gutierrez, H. M.; Schallhorn, P. A.; Marsell, B.; Roth, J.; Moder, J. P.: "Results of microgravity fluid dynamics captured with the SPHERES-Slosh experiment", Acta Astronautica, Vol. 111, pp. 280-290, 2015.

[56] Liu, J.; Li, X.; Li, L.; Chen, J.; Lin, X.: "Testing liquid distribution in a vane-type propellant tank under conditions of microgravity using a drop tower test", International Journal of Aerospace Engineering, Vol. 2020, Art. ID 6402083, 2020. https://doi.org/10.1155/2020/6402083

[57] Vreeburg, J. P.: "Spacecraft maneuvers and slosh control", IEEE Control Systems Magazine, Vol. 25, No. 3, pp. 12-16, 2005. https://doi.org/10.1109/MCS.2005.1432593

[58] Bulian, G.; Souto-Iglesias, A.; Delorme, L.; Botia-Vera, E.: "Smoothed particle hydrodynamics (SPH) simulation of a tuned liquid damper with angular motion", Journal of Hydraulic Research, Vol. 48, sup1, pp. 28–39, 2010. https://doi.org/10.3826/JHR.2010.0001

[59] NASA: "Slosh Suppression", NASA Space Vehicle Design Criteria, NASA SP-8031, 1969.

[60] Strahan, A.; Hernandez, H.: "Slosh Baffle Design and Test for Spherical Liquid Oxygen and Liquid Methane Propellant Tank for a Lander", in 47th AIAA/ASME/SAE/ASEE Joint Propulsion Conference & Exhibit, AIAA 2011-5633, 2011. https://doi.org/10.2514/6.2011-5633

[61] Miles, J. W.: "Ring damping of free surface oscillations in a circular tank", Journal of

Applied Mechanics, Vol. 25, No. 2, pp. 274-276, 1958. https://doi.org/10.1115/1.4011756

[62] West, J.; Yang, H. Q.; Brodnick, J.; Sansone, M.; Westra, D.: "Extension of Miles Equation for Ring Baffle Damping Predictions to Small Slosh Amplitudes and Large Baffle Widths", NASA/TM-2017-219572, 2016.

[63] Stephens, D. G.; Leonard, H. W.: "An experimental investigation of the damping of liquid oscillations in an oblate spheroidal tank with and without baffles", NASA Technical Note TN D-808, 1961.

[64] Chintalapati, S.; Kirk, D.; Faure, J.; Zhou, R.; Vergalla, M.; Gutierrez, H.: "Parametric study of a propellant tank slosh baffle", in 44th AIAA/ASME/SAE/ASEE Joint Propulsion Conference & Exhibit, AIAA 2008-4750, 2008. https://doi.org/10.2514/6.2008-4750

[65] Brooks, G. W.; Stephens, D. G.: "Flexible ring baffles for damping liquid slosh", NASA Technical Reports Server, NTRS 19680000064, 1968.

[66] Wang, J. D.; Zhou, D.; Liu, W. Q.: "Sloshing of Liquid in Rigid Cylindrical Container with a Rigid Annular Baffle. Part I: Free Vibration", Shock and Vibration, Vol. 19, No. 6, pp. 1185-1203, 2012. https://doi.org/10.3233/SAV-2012-0681

[67] Jaekle, D. E., Jr.: "Propellant management device conceptual design and analysis - galleries", in 33rd Joint Propulsion Conference and Exhibit, AIAA 1997-2811, 1997. https://doi.org/10.2514/6.1997-2811

[68] Jaekle, D. E.: "Propellant management device conceptual design and analysis – traps and troughs", in 31st Joint Propulsion Conference and Exhibit, AIAA 1995-2531, 1995. https://doi.org/10.2514/6.1995-2531

[69] Behruzi, P. et al.: "Future Propellant Management Device Concepts for Restartable Cryogenic Upper Stages", in 43rd AIAA/ASME/SAE/ASEE Joint Propulsion Conference & Exhibit, AIAA 2007-5498, 2007. https://doi.org/10.2514/6.2007-5498

[70] Debreceni, M. et al.: "Design and development of a communications satellite propellant tank", in 31st Joint Propulsion Conference and Exhibit, AIAA 1995-2529, 1995. https://doi.org/10.2514/6.1995-2529

[71] Vasireddy, S.; Camarotti, C.; Hartwig, J. et al.: "Liquid Acquisition Device Screen Compliance Experiments with Rectangular Geometry for Microgravity Applications", Microgravity Science and Technology, Vol. 34, Art. no. 2, 2022. https://doi.org/10.1007/s12217-021-09921-4

[72] Wang, Z.; Yang, G.; Wang, Y.; Jin, X.; Zhuan, R.; Zhang, H.; Wu, J.: "A three-dimensional flow model of screen channel liquid acquisition devices for propellant management in microgravity", npj Microgravity, Vol. 8, Art. no. 34, 2022. https://doi.org/10.1038/s41526

-022-00216-5

[73] Weislogel, M. M.; Graf, J. C.; Wollman, A. P. et al.: “How advances in low-g plumbing enable space exploration”, npj Microgravity, Vol. 8, Art. no. 16, 2022. https://doi.org/10.1038/s41526-022-00201-y

[74] Weislogel, M. M.; Thomas, E. A.; Graf, J. C.: “A Novel Device Addressing Design Challenges for Passive Fluid Phase Separations Aboard Spacecraft”, Microgravity Science and Technology, Vol. 21, pp. 257–268, 2009. https://doi.org/10.1007/s12217-008-9091-7

[75] McCraney, J.; Weislogel, M.; Steen, P.: “The draining of capillary liquids from containers with interior corners aboard the ISS”, npj Microgravity, Vol. 7, Art. no. 45, 2021. https://doi.org/10.1038/s41526-021-00173-5

[76] Weislogel, M. M.; Collicott, S. H.: “Capillary rewetting of vaned containers: spacecraft tank rewetting following thrust resettling”, AIAA Journal, Vol. 42, No. 12, pp. 2551-2561, 2004. https://doi.org/10.2514/1.3394

[77] Liu, J. et al.: “Numerical investigation of performance of vane-type propellant management device by VOF methods”, IOP Conference Series: Materials Science and Engineering, Vol. 72, No. 4, p. 042041, 2015. https://doi.org/10.1088/1757-899X/72/4/042041

[78] He, J. et al.: “Liquid directional transport surface applied to the spacecraft fluid management system: Fundamentals and prospect analysis”, Droplet, Vol. 4, No. 1, p. e165, 2025. https://doi.org/10.1002/dro2.165

[79] Konar, T.; Ghosh, A. D.: “Flow Damping Devices in Tuned Liquid Damper for Structural Vibration Control: A Review”, Archives of Computational Methods in Engineering, Vol. 28, pp. 2195–2207, 2021. https://doi.org/10.1007/s11831-020-09450-0

[80] Jetzschmann, C. et al.: “Model Based Active Slosh Damping Experiment”, arXiv preprint arXiv:1801.10017, 2018. https://doi.org/10.48550/arXiv.1801.10017

[81] Gligor, D. et al.: “Sloshing mitigation in microgravity with moving baffles”, Acta Astronautica, Vol. 219, pp. 370–382, 2024. https://doi.org/10.1016/j.actaastro.2024.03.047

[82] Tang, J.; Liang, Z.; Zheng, K.; Zheng, P.: “Design and simulation of anti-sloshing baffles applied to detumbling payload propellant tanks”, Journal of Physics: Conference Series, Vol. 2633, p. 012014, 2023. https://doi.org/10.1088/1742-6596/2633/1/012014

[83] Romero-Calvo, Á.; Hermans, T. H. J.; Cano-Gómez, G.; Parrilla Benítez, L.; Herrada Gutiérrez, M. Á.; Castro-Hernández, E.: “Ferrofluid dynamics in microgravity conditions”, in Proceedings of the 2nd Symposium on Space Educational Activities, Budapest, Hungary, 2018. https://doi.org/10.13140/RG.2.2.25110.45125

[84] Romero-Calvo, Á.; Cano-Gómez, G.; Castro-Hernández, E.; Maggi, F.: “Free and forced oscillations of magnetic liquids under low-gravity conditions", Journal of Applied Mechanics, Vol. 87, No. 2, p. 021004, 2020. https://doi.org/10.1115/1.4045620

[85] Romero-Calvo, Á.; Cano-Gómez, G.; Hermans, T. H. J.; Parrilla Benítez, L.; Herrada Gutiérrez, M. Á.; Castro-Hernández, E.: "Total magnetic force on a ferrofluid droplet in microgravity", Experimental Thermal and Fluid Science, Vol. 117, p. 110124, 2020. https://doi.org/10.1016/j.expthermflusci.2020.110124

[86] Romero-Calvo, Á.; García-Salcedo, A. J.; Garrone, F.; Rivoalen, I.; Cano-Gómez, G.; Castro-Hernández, E.; Herrada, M. Á.; Maggi, F.: "StELIUM: A student experiment to investigate the sloshing of magnetic liquids in microgravity", Acta Astronautica, Vol. 173, pp. 344–355, 2020. https://doi.org/10.1016/j.actaastro.2020.04.013

[87] Romero-Calvo, Á. et al.: "Lateral and Axisymmetric Ferrofluid Oscillations in a Cylindrical Tank in Microgravity", AIAA Journal, Vol. 60, No. 7, pp. 4147–4158, 2022. https://doi.org/10.2514/1.J061351

[88] Romero-Calvo, Á. et al.: "Novel propellant settling strategies for liquid rocket engine restart in microgravity", Acta Astronautica, Vol. 202, pp. 783-796, 2022. https://doi.org/10.1016/j.actaastro.2022.10.012

[89] Hart, S.; Romero-Calvo, Á.: "Thermoelectromagnetic smallSat propellant positioning", Acta Astronautica, Vol. 215, pp. 415-425, 2024. https://doi.org/10.1016/j.actaastro.2023.11.007

[90] Qi, R.; Wang, L.; Jin, J. et al.: "An embedded piezoelectric actuator for active vibration control: Concept, modeling, simulation, and investigation", Chinese Journal of Aeronautics, Vol. 38, No. 4, pp. 182–196, 2025. https://doi.org/10.1016/j.cja.2024.103345

[91] Hervas, J. R.; Reyhanoglu, M.: "Thrust-vector control of a three-axis stabilized upper-stage rocket with fuel slosh dynamics", Acta Astronautica, Vol. 98, pp. 120-127, 2014. https://doi.org/10.1016/j.actaastro.2014.01.022

[92] Hung, R. J.; Pan, H. L.: "Sloshing dynamics-modulated fluid angular momentum and moment fluctuations driven by orbital gravity gradient and jitter accelerations in microgravity", Applied Scientific Research, Vol. 54, pp. 51-68, 1995. https://doi.org/10.1007/BF01666802

[93] Shekhawat, A.; Nichkawde, C.; Ananthkrishnan, N.: "Modelling and stability analysis of coupled slosh-vehicle dynamics in planar atmospheric flight", in 44th AIAA Aerospace Sciences Meeting and Exhibit, Reno, NV, AIAA 2006-427, 2006. https://doi.org/10.2514/6.2006-427

[94] Zhang, H.; Wang, Z.: "Attitude control and sloshing suppression for liquid-filled spacecraft in the presence of sinusoidal disturbance", Journal of Sound and Vibration, Vol. 384, pp. 34–52, 2016. https://doi.org/10.1016/j.jsv.2016.08.001

[95] Thompson, J. W.; O'Connor, W. J.: "Wave-based attitude control of spacecraft with fuel slosh dynamics", Journal of Mechanical Engineering, Vol. 62, No. 1, pp. 15–26, 2016. https://doi.org/10.1515/meceng-2016-0015

[96] Leiter, N.; Priel, A.; Yaniv, O.: "Robust spacecraft attitude control under multi-tank sloshing disturbances during orbit correction maneuvers", in 27th Mediterranean Conference on Control and Automation (MED), pp. 450-455, 2019. https://doi.org/10.1109/MED.2019.8798502

[97] Angeletti, F. et al.: "Learning-based Control of a Spacecraft with Sloshing Propellant", Aerotecnica Missili & Spazio, Vol. 99, pp. 245-256, 2020. https://doi.org/10.1007/s42496-020-00033-7

[98] Lee, A. Y.; Stupnik, J.: "In-Flight Characterization of the Cassini Spacecraft Propellant Slosh Modes", Journal of Spacecraft and Rockets, Vol. 53, No. 6, pp. 1179-1188, 2016. https://doi.org/10.2514/1.A33636

[99] Guan, J. H.; Magoon, C. W.; Durey, M.; Camassa, R.; Sáenz, P. J.: "Traveling Faraday waves", Physical Review Fluids, Vol. 8, No. 11, p. 110501, 2023. https://doi.org/10.1103/PhysRevFluids.8.110501

[100] Douady, S.: "Experimental study of the Faraday instability", Journal of Fluid Mechanics, Vol. 221, pp. 383-409, 1990. https://doi.org/10.1017/S0022112090003603

[101] Martín López, Á. L.; Sánchez-Ojeda, I.; Gonzalez, L.: "Experimental study of different sloshing regimes in a horizontal cylindrical tank under lateral excitation", European Journal of Mechanics - B/Fluids, Vol. 119, p. 204551, 2026. https://doi.org/10.1016/j.euromechflu.2026.204551

[102] Colville, S.; Ransley, E.; Gambioli, F.; Lee, Y. C.; Greaves, D.: "Fluid response of sloshing in a horizontal cylinder due to horizontal excitation", in Proceedings of the International Offshore and Polar Engineering Conference, pp. 1025–1032, 2023. ISBN: 978-1-880653-80-7.

[103] Colville, S. W.; Scolan, Y.-M.; Gambioli, F.; Greaves, D.; Ransley, E.; Lee, Y. C.: "Faraday waves and period tripling in a horizontal circular tank", Journal of Fluid Mechanics, Vol. 1006, p. A4, 2025. https://doi.org/10.1017/jfm.2025.16

[104] Roux, M. C. N.; Meunier, B. A. H.; Mari, D.: "Study of Faraday waves in tanks in presence of polystyrene bead layers", Emergent Scientist, Vol. 7, p. 2, 2023. https://doi.org/10.1051/emsci/2023001

[105] Ibrahim, R. A.: "Recent advances in vibro-impact dynamics and collision of ocean vessels", Journal of Sound and Vibration, Vol. 333, No. 23, pp. 5900-5916, 2014. https://doi.org/10.1016/j.jsv.2014.02.006

[106] Isaac, C. W.; Wrona, S.; Pawelczyk, M.; Karimi, H. R.: "Modelling vibro–acoustic response of lightweight square aluminium panel influenced by sound source locations for active control", Scientific Reports, Vol. 12, Art. no. 10727, 2022. https://doi.org/10.1038/s41598-022-14951-y

[107] Lukovsky, I. A.; Timokha, A. N.: "Sound Effect on Dynamics and Stability of Fluid Sloshing in Zero Gravity", International Journal of Fluid Mechanics Research, Vol. 28, No. 1–2, pp. 19–41, 2001. ISSN 1064-2285

Abbreviations

3D	Three-Dimensional
BEM	Boundary Element Method
Bo	Bond number ($\text{Bo} = \Delta\rho\, g\, L^2/\gamma$)
CFD	Computational Fluid Dynamics
d	Liquid depth above baffle plane
DCA	Dynamic Contact Angle
DG	Discontinuous Galerkin
DLR	German Aerospace Center (Deutsches Zentrum für Luft- und Raumfahrt)
D_p	Effective screen pore diameter ($D_{p,293\text{K}}$)
ESA	European Space Agency
FARE	Fluid Acquisition and Resupply Experiment
FDD	Flow Damping Device
FDM	Finite Difference Method
FEA	Finite Element Analysis
FEM	Finite Element Method
f_{fs}	Free surface slosh disturbance force
FFT	Fast Fourier Transform
FiPS	Final Phase Simulator
FLUIDICS	Fluid Dynamics in Space
f_{rs}	Rigid container inertia force
FVM	Finite Volume Method
g	Gravitational acceleration
GNC	Guidance, Navigation, and Control
GPU	Graphics Processing Unit
h	SPH smoothing length
ISS	International Space Station
L	Characteristic container length scale
LAD	Liquid Acquisition Device
LBM	Lattice Boltzmann Method
LCH_4	Liquid Methane
LDD	Lagrangian Differencing Dynamics
LH_2	Liquid Hydrogen
LN_2	Liquid Nitrogen
LNG	Liquefied Natural Gas
LOX	Liquid Oxygen
m	Circumferential wave number
m_0	Fixed mass in equivalent mechanical model

m_n	Modal sloshing mass of n-th mode
MP2	Magnetic Positive Positioning
NASA	National Aeronautics and Space Administration
NS	Navier–Stokes
PMD	Propellant Management Device
R	Tank radius
$\mathbf{r}, \mathbf{r}'$	Position vectors in continuum domain
RANS	Reynolds-Averaged Navier–Stokes
s	Laplace transform variable
SEM	Spectral Element Method
SloshSat-FLEVO	Slosh Satellite – Facility for Liquid Experimentation and Verification in Orbit
SmallSat	Small Satellite
SPH	Smoothed Particle Hydrodynamics
SPHERES	Synchronized Position Hold, Engage, Reorient, Experimental Satellites
TLCD	Tuned Liquid Column Damper
TLD	Tuned Liquid Damper
TMD	Tuned Mass Damper
VOF	Volume of Fluid
w	Annular baffle width
W	SPH smoothing kernel interpolation function
Z_n	Generalized modal displacement coordinate
γ	Liquid–gas surface tension
ζ	Viscous damping ratio (ζ_n)
η	Liquid free surface elevation
η_0	Free surface wave amplitude at container wall
θ_C	Contact angle at liquid–solid–gas interface
ΔP_{bp}	Bubble-point pressure (ΔP_{BP})
$\Delta\rho$	Density difference between liquid and ullage gas
ω	Natural angular slosh frequency (ω_n, ω_m)

Abstract

Propellant sloshing, the capillary-dominated oscillation of liquid inside partially filled tanks, presents a major fluid–structure–control challenge in spaceflight. In microgravity, the governing physics shifts away from gravity-restored motion: surface tension becomes the primary restoring mechanism, the free surface forms a curved, Bond-number-dependent meniscus, and minor vehicle maneuvers can trigger large-amplitude, weakly damped oscillations that disturb attitude control and structural stability. Aerospace engineering has established effective passive mitigation methods, including annular ring baffles, flexible dampers, and surface-tension propellant management devices (PMDs). Over the last two decades, active and semi-active approaches have also emerged, spanning force-feedback hexapod platforms, moving baffles, magnetic ferrofluid positioning, and piezoelectric structural damping. This review surveys passive, active, and vibroacoustic methods for low-gravity slosh control, grounded in equivalent mechanical modeling and capillary hydrodynamics. It examines microgravity experimental facilities (drop towers, parabolic flights, ISS testbeds) and computational tools (VOF, RANS, SPH). Based on the limitations of existing active techniques, this review proposes acoustically mediated active slosh control via ultrasonic radiation pressure as a promising, underexplored, and technically viable direction for doctoral research.

Keywords: hydrodynamics, propellant sloshing, microgravity, active slosh control

Prošireni sažetak

Gibanje tekućine u pokretnim spremnicima važno je za projektiranje sigurnijih vozila, brodova i konstrukcija. Kada tekućine zapljuskuju unutar djelomično napunjenih spremnika, rezultirajuće gibanje izravno remeti dinamiku vozila. Ovaj problem je dobro poznat u mnogim inženjerskim područjima, uključujući projektiranje spremnika za gorivo zrakoplova i raketa, izgradnju brodova i drugih vozila. Pljuskanje može proizvesti nestabilne sile i momente prevrtanja na strukturi spremnika, izravno utječući na središte mase i kretanje vozila. Na Zemlji gravitacija regulira zapljuskivanje, gradijent hidrostatskog tlaka vuče istisnutu tekućinu natrag prema ravnoj ravnoteži, dok površinska napetost djeluje samo kao lokalna korekcija u blizini stijenki spremnika. U režimu gdje je Bondov broj nizak ($Bo \leq 1$), kapilarne sile mogu postati veće od gravitacijskih sila stoga inercija ostaje važna za dinamički odziv tekućine, dok viskozni učinci doprinose disipaciji energije i prigušenju. Umjesto ravnog međupovršinskog oblika, tekućine se penju uz stijenke spremnika, zarobljavaju mjehuriće plina i preorijentiraju se tijekom manevara svemirske letjelice. Budući da modeli ravnog međupovršinskog oblika pretpostavljaju uvjete Zemljine gravitacije, njihove pretpostavke za predviđanje gibanja tekućine u uvjetima mikrogravitacije mogu postati neadekvatne. Upravljanje zapljuskivanjem pri niskoj gravitaciji stoga je preraslo u multidisciplinarno područje koje povezuje kapilarnu hidrodinamiku, strukturnu dinamiku, teoriju preciznog upravljanja i aktivnu aktuaciju. Zapisi o letovima dokumentiraju nekoliko kritičnih slučajeva. Tijekom spuštanja lunarnog modula Apollo 11, pomak orijentacije uzrokovan zapljuskivanjem više je puta komplicirao ponovna pokretanja motora i povećavao potrošnju goriva. Ovo pitanje motiviralo je karakterizaciju ponašanja dinamike zapljuskivanja u različitim režimima leta, korištenjem eksperimentalnih testova i numeričkih simulacija. Studije analiziraju zapljuskivanje u sfernim tankovima s vodom i tekućim dušikom, kriogeno zapljuskivanje pogonskog goriva u cilindričnim spremnicima pod tlakom, analitičku analizu skladištenja pogonskog goriva u svemiru i ispitivanje zapljuskivanja vodika velikih razmjera. Eksperimentalne i numeričke studije poboljšale su predviđanja poremećaja zapljuskivanja i prigušenja u tankovima. Ovaj pregled ispituje fizičke mehanizme, pasivne uređaje i metode aktivnog upravljanja zapljuskivanja u tankovima u uvjetima mikrogravitacije. Odjeljak 2 ispituje kapilarnu hidrodinamiku, mehaniku kontaktnih linija i ekvivalentne mehaničke modele koji se koriste u kontroli leta. Odjeljak 3 pregledava pasivne tehnologije, uključujući prstenaste pregrade, jednadžbe prigušenja, uređaje za upravljanje pogonskim gorivom površinske napetosti (PMD) i podešene tekuće prigušivače. Odjeljak 4 istražuje strategije aktivnog upravljanja, obuhvaćajući platforme s povratnom vezom sile, mobilne pregrade, pozicioniranje magnetskog ferofluida, piezoelektrične pretvarače i zakone upravljanja položajem spojenih svemirskih letjelica. Odjeljak 5 raspravlja o vibroakustičnim fenomenima, s naglaskom na tlak akustičnog zračenja, ultrazvučnu manipulaciju i razliku između strukturne akustike i aktuacije na fluidnom sučelju. Završni odjeljak donosi zaključke, ključne istraživačke nedostatke i predstavlja istraživački prijedlog za akustičnu kontrolu zapljuskivanja.

Ključne riječi: hidrodinamika, zapljuskivanje fluida, mikrogravitacija, aktivna kontrola zapljuskivanja